Synthesis, Structures and Co-Crystallizations of Perfluorophenyl Substituted β-Diketone and Triketone Compounds

Takumi Kusakawa [1], Shunichiro Sakai [2], Kyosuke Nakajima [2], Hidetaka Yuge [2], Izabela I. Rzeznicka [1] and Akiko Hori [1,*]

[1] Graduate School of Engineering and Science, Shibaura Institute of Technology, Fukasaku 307, Minuma-ku, Saitama 337-8570, Japan; mc18014@shibaura-it.ac.jp (T.K.); izabela@shibaura-it.ac.jp (I.I.R.)

[2] Department of Chemistry, School of Science, Kitasato University, Kitasato 1-15-1, Minami-ku, Sagamihara 252-0373, Japan; sc09336z@st.kitasato-u.ac.jp (S.S.); ms12815m@st.kitasato-u.ac.jp (K.N.); yuge@kitasato-u.ac.jp (H.Y.)

* Correspondence: ahori@shibaura-it.ac.jp; Tel.: +81-42-720-6350

Abstract: Perfluorophenyl-substituted compounds, 3-hydroxy-1,3-bis(pentafluorophenyl)-2-propen-1-one (H**1**) and 1,5-dihydroxy-1,5-bis(pentafluorophenyl)-1,4-pentadien-3-one (H$_2$**2**), were prepared in 56 and 30% yields, respectively, and only the enol forms were preferentially obtained among the keto-enol tautomerism. Molecular conformations and tautomerism of the fluorine-substituted compounds were certified based on X-ray crystallographic studies and density functional calculations. The solvent dependency of the absorption spectra was only observed for the fluorinated compounds. The compounds H**1** and H$_2$**2** quantitatively formed co-crystals with the corresponding non-perfluorinated compounds, dibenzoylmethane (H**3**) and 1,5-dihydroxy-1,5-diphenyl-1,4-pentadien-3-one (H$_2$**4**), respectively, through the arene–perfluoroarene interaction to give the 1:1 co-crystals H**1**•H**3** and H$_2$**2**•H$_2$**4**, which were characterized by X-ray crystallographic and elemental analysis studies.
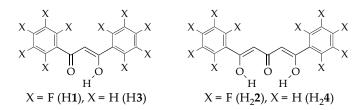
Keywords: co-crystals; electrostatic interactions; fluorine; keto-enol form

1. Introduction

Fluorine-substituted organic molecules are being widely explored by materials scientists in various applications encompassing battery, catalysis, and many other technological fields [1–5]. Ring fluorination dramatically changes molecular characteristics through intramolecular electron withdrawing nature and intermolecular electrostatic interactions. One of the unique properties of perfluoroaromatic compounds is the opposite quadrupole moment [6], which is positive for hexafluorobenzene, 31.7×10^{-40} C m^2, and negative for benzene, -29.0×10^{-40} C m^2 [7,8]. Thus, unique π-interactions, such as arene–perfluoroarene [9–27] and CH···F [28–30], are observed in the crystals of perfluorinated compounds and co-crystals containing perfluorinated and non-perfluorinated aromatic compounds. The co-crystals have alternating layered structures and are found to possess unique molecular recognition capabilities [10]. In this area, we have been interested in the perfluoroarene coordination compounds and their molecular self-assembled systems for a decade; e.g., bis[bis(pentafluorobenzoyl)]copper(II), [Cu(**1**)$_2$], was prepared and applied to metal-ordered co-crystals with unique one-dimensional metal chains [31] and several guest encapsulations in the crystal states [32–35]. However, the corresponding ligand, 3-hydroxy-1,3-bis(pentafluorophenyl)-2-propen-1-one (H**1**) (Scheme 1) [36], which is a unique target for the fluorine-substituted dibenzoylmethane [37], has never been characterized by crystallographic studies, whereas the corresponding coordination complexes have been reported. This fact encouraged us to characterize

and develop the structure of the perfluorinated compound H**1** and also prepare the expanded triketone-type compound H$_2$**2**, of which both structures always involve the problems of keto-enol tautomerism [38–47]. In this study, we investigated the molecular structures and the supramolecular associations of H**1** and H$_2$**2** in the solution and solid states, which further co-crystallize with the corresponding non-perfluorinated compounds H**3** and H$_2$**4**, respectively, to give the unique 1:1 co-crystals of H**1**• H**3** and H$_2$**2**•H$_2$**4**.

X = F (H**1**), X = H (H**3**)　　　　　　　X = F (H$_2$**2**), X = H (H$_2$**4**)

Scheme 1. Molecular structures of perfluorinated compounds, H**1** and H$_2$**2,** and non-perfluorinated compounds, H**3** and H$_2$**4**.

2. Materials and Methods

2.1. General

All the chemicals were of reagent grade and used without further purification. Non-perfluorinated compounds H**3** and H$_2$**4** were commercially available. The ^{1}H NMR spectral data were recorded by a Bruker DRX600 (600 MHz) or JEOL ECS400 (400 MHz) spectrometer. The melting points were determined by a Yanako MP-500D melting point apparatus. The infrared spectra were recorded by a Shimadzu IR 8400s using a KBr disk. The electronic absorption spectra were recorded by a JASCO V-660 spectrometer. The results of the elemental analysis (EA) of C and H were determined by a Perkin-Elmer PE2400 analyzer. The DFT calculations were performed by the Spartan'16 package with B3LYP/6-31G* [48,49].

2.2. Synthesis of H1 and H$_2$2

The synthesis of 3-hydroxy-1,3-bis(pentafluorophenyl)-2-propen-1-one (H**1**) was previously reported [36,50]. Typically, pentafluorobenzoyl chloride and vinyl acetate were combined in 1,1,2,2-tetrachloroethane in the presence of anhydrous AlCl$_3$. The reaction mixture was separated by a column chromatography (silica, benzene). The H**1** product was obtained at R_f = 0.8, and two other byproducts corresponding to the aluminum complex and acethylpentafluorobenzoylmethane were obtained at R_f = 0.9 and 0.5, respectively. With sufficient acid treatment after the reaction, the H**1** product was preferentially obtained instead of the corresponding aluminum (III) complex. Compound H**1** was further purified by gel permeation chromatography (GPC) and recrystallized from an ethanol solution to give colorless prismatic crystals with the constant melting point of 83–84 °C in 56% yield. ^{1}H NMR (600 MHz, CDCl$_3$): δ 15.12 (s, OH), 6.26 (s, CH). ^{13}C NMR (150 MHz, CDCl$_3$): δ 177.0 (CO), 144.9 (d(m), J = 257 Hz, C$_6$F$_5$), 143.2 (d(m), J = 257 Hz, C$_6$F$_5$), 137.9 (d(m), J = 257 Hz, C$_6$F$_5$), 111.3 (m, C$_6$F$_5$), 106.3 (CH). IR (KBr disk, cm^{-1}): 3457, 3144, 2926, 1651, 1593, 1524, 1497, 1335, 1319, 1206, 1180, 1099, 995, 932, 827, 642. EA: Calcd. for C$_{15}$H$_2$F$_{10}$O$_2$ (%): C, 44.58; H, 0.50. Found: C, 44.65; H, 0.38.

1,5-Dihydroxy-1,5-bis(pentafluorophenyl)-1,4-pentadien-3-one (H$_2$**2**) was prepared by adding a solution of hexamethyldisilazine (7.2 mL, 32 mmol) in dry tetrahydrofuran (THF, 15 mL) to n-BuLi (19.4 mL, 32 mmol, hexane) at 0 °C under an N$_2$ atmosphere with continuous stirring for 15 min. Subsequently, freshly distilled acetone (0.75 mL, 11 mmol), dissolved in 15 mL of THF, was dropwise added to the mixture, then a solution of methylpentafluorobenzoate (5 mL, 22 mmol) in THF (25 mL) was added. The mixture was stirred for 20 h at room temperature. During the stirring, the solution color changed from colorless to dark orange. Subsequently, the mixture was added to an aqueous solution of 3M HCl (100 mL), neutralized by NaHCO$_3$, and extracted with diethylether. The obtained

mixture was purified by column chromatography (silica, CH_2Cl_2). The first product was assigned to methylpentafluorobenzoate (R_f = 0.7), and the second product with R_f = 0.5 was characterized as H$_2$**2**. Compound H$_2$**2** was further purified by GPC and recrystallized from ethanol to give yellow prismatic crystals. Yield 30%. mp 87–88 °C. ^{1}H NMR (600 MHz, CDCl$_3$, TMS): δ 14.26 (s, 2H, OH), 5.73 (s, 2H, CH). ^{13}C NMR (150 MHz, CDCl$_3$): δ 194.0 (COH), 164.4 (CO), 144.8 (d(m), J = 254 Hz, C_6F_5), 142.6 (d(m), J = 254 Hz, C_6F_5), 137.9 (d(m), J = 254 Hz, C_6F_5), 110.0 (m, C_6F_5), 104.5 (CH). IR (KBr disk, cm^{-1}): 3148, 1651, 1607, 1522, 1495, 1377, 1196, 1167, 1084, 1011, 837, 716. EA: Calcd. for $C_{17}H_4F_{10}O_3$ (%): C, 45.76; H, 0.90. Found: C, 45.84; H 0.83.

2.3. Co-Crystallizations of H1●H3 and H$_2$2●H$_2$4

The perfluorinated compound and the corresponding non-perfluorinated compound were completely dissolved in EtOH, then combined for co-crystallization. Stoichiometric co-crystals grew slowly under slow solvent evaporation conditions.

Co-crystal H**1**●H**3**. The crystal was obtained as a colorless prismatic. Isolated yield: 74%. mp 106–108 °C. IR (KBr disk, cm^{-1}): 3457, 3119, 3082, 1672, 1653, 1524, 1497, 1371, 1107, 993, 768, 691. EA: Calcd. for $C_{30}H_{14}F_{10}O_4$ (%): C, 57.34; H, 2.25. Found: C, 57.39; H 1.88.

Co-crystal H$_2$**2**●H$_2$**4**. The crystal was obtained as a yellow prismatic. Isolated yield: 94%. Mp 125–126 °C. IR (KBr disk, cm^{-1}): 1653, 1609, 1520, 1493, 1157, 1082, 1007, 982, 824, 775, 691. EA: Calcd. for $C_{34}H_{18}F_{10}O_6$ (%): C, 57.32; H, 2.55. Found: C, 57.05; H 2.46.

2.4. Crystal Structure Determination

The single crystal X-ray structures were determined by a Bruker SMART APEX CCD diffractometer with a graphite monochrometer and Mo$K\alpha$ radiation (λ = 0.71073 Å) generated at 50 kV and 30 mA. All the crystals were coated by paratone-N oil and measured at 120 K. SHELXT program was used for solving the structures [51]. Refinement and further calculations were carried out using SHELXL [52]. The crystal data and structure refinement of the perfluorinated compounds (H**1** and H$_2$**2**) and their co-crystals (H**1**●H**3** and H$_2$**2**●H$_2$**4**) are summarized in Table 1. CCDC 1827049 (H**1**), 1827050 (H$_2$**2**), 1827051 (H**1**●H**3**), and 1827052 (H$_2$**2**●H$_2$**4**) contain the supplementary crystallographic data for this paper. These data can be obtained free of charge via http://www.ccdc.cam.ac.uk/conts/retrieving.html.

Table 1. Crystal data and structure refinement for H**1**, H$_2$**2**, H**1**●H**3**, and H$_2$**2**●H$_2$**4**.

	H**1**	H$_2$**2**	H**1**●H**3**	H$_2$**2**●H$_2$**4**
Chemical formula	$C_{15}H_2F_{10}O_2$	$C_{17}H_4F_{10}O_3$	$C_{30}H_{14}F_{10}O_4$	$C_{34}H_{18}F_{10}O_6$
Formula weight	404.17	446.20	628.41	712.48
Crystal system	monoclinic	monoclinic	monoclinic	monoclinic
Space group	$P2_1/n$	$P2_1/c$	$P2_1/c$	$P2_1/c$
a [Å]	10.3800(11)	17.4336(12)	13.4003(10)	15.7397(14)
b [Å]	5.6285(6)	4.9910(3)	7.0784(5)	7.0887(6)
c [Å]	23.196(3)	18.3069(12)	26.1345(18)	25.835(2)
β [°]	94.2233(12)	106.929(1)	95.2152(8)	98.842(1)
V [Å^3]	1351.5(2)	1523.88(17)	2468.7(3)	2848.3(4)
Z	4	4	4	4
D_c [Mg m^{-3}]	1.986	1.945	1.691	1.662
μ [mm^{-1}]	0.223	0.213	0.162	0.156
$F(000)$	792	880	1264	1440
R_{int}	0.0240	0.0194	0.0238	0.0265
GOF	1.061	1.033	1.047	1.035
R [$(I) > 2\sigma(I)$]	0.0303	0.0301	0.0337	0.0334
wR ($F_o{}^2$)	0.0845	0.0849	0.0930	0.0952
CCDC No.	1827049	1827050	1827051	1827052

3. Results and Discussion

3.1. Enol-Type Structures of H1 and 2

Compounds H**1** and H$_2$**2** were prepared by using previously described protocols, purified by column chromatography, GPC, and recrystallized to give pure single products. The ^{1}H NMR results of both structures in CDCl$_3$ clearly suggested enol-type structures. The ^{1}H NMR spectrum of H**1** in CDCl$_3$ shows only two single peaks at δ 15.12 (OH) and 6.26 (CH), indicating the enolic form; the enol tautomeric species generally contains a hydrogen bonded ring comprised of two equivalent structures with C_s symmetry connected through a transition state with C_{2v} symmetry [38]. The ^{1}H NMR spectrum of H$_2$**2** in CDCl$_3$ also shows two single peaks at δ 14.26 (OH) and 5.73 (CH), indicating the highly symmetric structure of H$_2$**2**, while several keto- and enol-type corresponding isomers are expected. Single crystals of H**1** and H$_2$**2** were obtained from ethanol as colorless and pale yellow prismatic crystals, respectively, which were suitable for X-ray crystallographic studies.

The molecular structures in the single crystals of H**1** and H$_2$**2** are shown in Figure 1a,b, respectively, with the numbering schemes. In the crystal of H**1**, the whole structure is an asymmetric unit, that is distinguishable as the C_s structure; the bond lengths of O1-C7, C7-C8, C8-C9, and C9-O2 are 1.2636(17), 1.4246(18), 1.3722(18) and 1.3103(16) Å, respectively, showing the localization of the π-conjugated system in the O1=C7-C8=C9-O2 coordination sites. The hydrogen proton is close to O2 to give C_s symmetry of the hydrogen bonded ring, such as the β-diketonato moiety: The distance of O1$\cdots$O2 and the angle of O1$\cdots$H2-O2 are 2.4857(14) Å and 146°, respectively. The enol form, which means keto-enol type structure, is stabilized by intramolecular hydrogen bonds to form a six-membered ring structure of the β-ketonate O1-C7-C8-C9–O2-H2, indicating the same orientation of the corresponding non-perfluorinated H**3** [53]. This phenomenon is well known as a resonance-assisted hydrogen bond (RAHB) by Gilli et al. [40,41]. Two pentafluorophenyl rings are highly twisted to the ring; the dihedral angles between the two pentafluorophenyl rings and the β-ketonate six-membered ring are 25.47° and 49.29°: the torsion angles of C1-C6-C7-O1 and O2-C9-C10-C11 are 24.47(18)° and 47.80(17)°, respectively. The low planarity of the molecules was compromised due to the twisting induced by the steric hindrance between the fluorine at the o-positions of the pentafluorophenyl group and the hydrogen at the ketonate sites. The related dihedral angles between two phenyl rings and the β−ketonate six-membered ring of H**3** are 4.69° and 17.42°, showing a flatter structure [53].
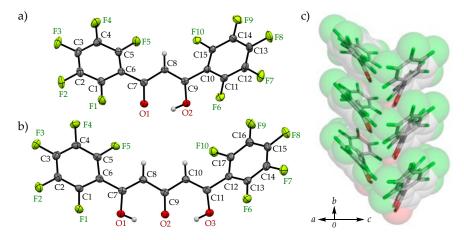

Figure 1. ORTEP drawings of the crystal structure of (**a**) H**1** and (**b**) H$_2$**2** at 120 K with 50% probability thermal ellipsoids and (**c**) the packing structure of H$_2$**2** viewed from the ac axis.

In the crystal of H$_2$**2**, O1 and O3 are also crystallographically independent. The bond lengths of O1-C7, O2-C9, and O3-C11 are 1.3363(15), 1.2784(15), and 1.3332(15) Å, respectively, indicating the enol-keto-enol type structure (proposed structure in Scheme 1). In this configuration, the bond lengths of C8-C9 and C9-C10 [1.4429(17) Å and 1.4403(16) Å] are longer than those of C7-C8 and C10-C11

[1.3617(17) Å and 1.3591(17) Å], which indicates that the localization of the π system with RAHB: the distances of O1···O2 and O2···O3 and the angles of O1-H1···O2 and O1···H3-O3 are 2.5565(13) Å, 2.5724(13) Å, 147°, and 146°, respectively. The two pentafluorophenyl rings of H_2**2** were highly twisted; the torsion angles of C1-C6-C7-O1 and O3-C11-C12-C13 are 22.61(16)° and −42.47(16)°, respectively. The corresponding torsion angles of the non-perfluorinated H_2**4** were flatter: 2.6(3)° and −21.4(3)° [54]. The enol structures based on the difference in the predominant bond length and the twist of the aromatic ring in the two compounds H**1** and H_2**2** are very similar. In the crystal packings of H**1** and H_2**2**, no remarkable π-π stacking was observed; the closest intermolecular distances between the two centroids of the pentafluorophenyl groups are sufficiently long (5.629 Å for H**1** and 4.991 Å for H_2**2**) due to the sliding orientations of the molecular planes along the *b* axis (Figure 1c).

3.2. UV-Vis Studies of the Perfluorinated Compounds

The UV-spectra for H**1**~H_2**4** were obtained in chloroform (CHCl$_3$), acetonitrile (CH$_3$CN), methanol (CH$_3$OH), and benzene (C$_6$H$_6$) solutions. The electronic absorption spectra of the four ligands in CHCl$_3$ are shown in Figure 2a. The maximum absorptions for H**1**, H**3**, H_2**2**, and H_2**4** are observed at 315, 343, 351, and 383 nm, respectively. The absorption bands of the perfluorinated ligands H**1** and H_2**2** (shown in solid lines) were broad and more symmetric but those of the non-perfluorinated ligands H**3** and H_2**4** (dashed lines) showed a peak shoulder on the side of the long wavelength (around 370 and 400 nm for H**3** and H_2**4**, respectively) [38]. The spectra of the triketonate ligands H_2**2** and H_2**4** (green lines) were about 36~40 nm red shifted in comparison to the corresponding diketone ligands H**1** and H**3** (black lines). The shift of each peak can be explained by expansion of the π-conjugated system. The spectra of the perfluorinated ligands H**1** and H_2**2** were blue shifted about 30 nm in comparison to the corresponding non-perfluorinated ligands H**3** and H_2**4**. The blue shift can be explained by a loss of planarity of both molecules [53,54]. The planarity of the molecules was compromised due to the twisting induced by the steric hindrance between the fluorine at the o-positions of the pentafluorophenyl group and the hydrogen at the ketonate sites, as suggested by the crystal structures.
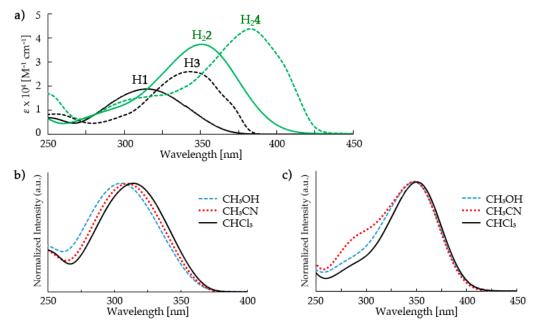

Figure 2. UV-Vis absorption spectra of (**a**) H**1**~H_2**4** in CHCl$_3$ solution (40 μM, 1 cm, rt.); and (**b**) H**1** and (**c**) H_2**2** in following solvents, CHCl$_3$, CH$_3$CN, and CH$_3$OH (1.0 mM, 1 mm, rt).

The maximum absorption wavelength and the shape of the spectrum of the perfluorinated ligands H**1** and H$_2$**2** were different depending on the solvent. The λ_{max} of H**1** in polar solvents, such as CH$_3$OH, was 305 nm and in the aprotic polar CH$_3$CN solvent, it was ca. 310 nm. The spectrum in the nonpolar CHCl$_3$ (λ_{max} 315 nm) was red shifted nearly 5 nm compared with that in the polar solvents as shown in Figure 2b. The λ_{max} of H$_2$**2** in the polar solvents was at 348–349 nm and slightly shifted from that in CHCl$_3$ (351 nm), and the intensity of the small shoulder peak around 280 nm increased in CH$_3$CN (Figure 2c). These solvent effects were not observed in the solution of H**3** and H$_2$**4**. The H**1** and H$_2$**2** absorption spectra in the benzene solution were almost the same as those observed in the CHCl$_3$ solution. This indicates that solvatochromism occurs only in the polar solvents.

3.3. Co-Crystallization by Arene-Perfluoroarene Interactions

The perfluorinated compound and the non-perfluorinated compound were combined to give 1:1 co-crystal. Typically, H**1** (121 mg, 0.30 mmol) in EtOH solution (2.5 mL) and H**3** (67 mg, 0.30 mmol) in EtOH solution (2.5 mL) were combined, then the mixture was slowly evaporated to give the colorless prismatic crystals H**1**•H**3**. Although the reaction proceeded quantitatively, the co-crystal was isolated before the filtrate disappeared so that the microcrystals did not stick to the precipitated single crystal. The H$_2$**2**•H$_2$**4** co-crystal was obtained as a yellow prismatic crystal using the same synthetic protocol. The results of the elemental analysis for H**1**•H**3** (C$_{30}$H$_{14}$F$_{10}$O$_4$) and H$_2$**2**•H$_2$**4** (C$_{34}$H$_{18}$F$_{10}$O$_6$) clearly showed that the crystallized products were pure with a 1:1 stoichiometry. The melting points of the co-crystals are expected to be higher than the single perfluorinated compounds: H**1**•H**3** (106 °C) > H**1** (83 °C) and H**3** (76 °C); H$_2$**2**•H$_2$**4** (125 °C) > H$_2$**2** (87 °C) and H$_2$**4** (107 °C).

The molecular structures of the co-crystals H**1**•H**3** and H$_2$**2**•H$_2$**4** are shown in Figure 3 with the corresponding numbering schemes. The major intra- and intermolecular interactions of H**1**•H**3** and H$_2$**2**•H$_2$**4** are summarized in Table 2. In Figure 3a, the co-crystal H**1**•H**3** is comprised of H**1** and H**3** in a 1:1 ratio. The mean planes of both molecular structures were highly overlapped by the arene–perfluoroarene interaction. The bond lengths of O1-C7 and O2-C9 in H**1** are 1.2607(17) Å and 1.3063(16) Å, respectively, and those of O3-C22 and O4-C24 in H3 are 1.2757(16) Å and 1.3054(16) Å, respectively, indicating the same type of π-conjugated structure of each molecular component. The two phenyl rings of H**3** were twisted to the plane of the β-diketonate moiety, and the torsional angles of the C1-C6-C7-O1 and O2-C9-C10-C11 are -30.64(19)° and 32.78(18)°, respectively. Similarly, the pentafluorophenyl groups of H**1** are twisted, producing 18.14(18)° and -12.71(18)° angles for C16-C21-C22-O3 and O4-C24-C25-C26, respectively.
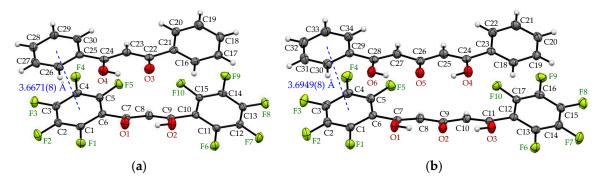

Figure 3. ORTEP drawings of the crystal structure of (**a**) H**1**•H**3** and (**b**) H$_2$**2**•H$_2$**4** with 50% probability thermal ellipsoids.

Table 2. Major intra- and intermolecular interactions of H**1**●H**3** and H$_2$**2**●H$_2$**4**.

	H**1**●H**3**	H$_2$**2**●H$_2$**4**
Intramolecular hydrogen bonds (O-H⋯O)	O1⋯O2, 2.5313(15) Å	O1⋯O2, 2.5495(14) Å O2⋯O3, 2.5811(14) Å
	O3⋯O4, 2.4882(15) Å	O4⋯O5, 2.5584(14) Å O5⋯O6, 2.5632(14) Å
	O1⋯H2-O2, 147°	O1-H1⋯O2, 147° O2⋯H3-O3, 146°
	O3⋯H4-O4, 148°	O4-H4⋯O5, 146° O5⋯H6-O6, 147°
Intermolecular hydrogen bonds (O-H⋯O)	not found	not found
Arene-perfluoroarene [$C_g(C_6F_5)\cdots C_g(C_6H_5)$]	π(C1-6)⋯π(C29-34), 3.6671(8) Å π(C10-15)⋯π(C16-21), 4.1008(9) Å	π(C1-6)⋯π(C29-34), 3.6949(8) Å π(C12-17)⋯π(C18-23), 4.0439(8) Å
C-F⋯π [C-F⋯$C_g(C_6F_5)$]	C4-F4⋯π(C29-34), 3.4806(11) Å C14-F9⋯π(C16-21), 3.2877(11) Å C15-F10⋯π(C16-21), 3.2364(10) Å	C4-F4⋯π(C29-34), 3.4959(11) Å C16-F9⋯π(C18-23), 3.2621(11) Å C17-F10⋯π(C18-23), 3.3073(11) Å

Parts of the packing structure of H**1**●H**3** are shown in Figure 4. The alternate stacking of the two compounds was observed along the *b* axis with alternating H**1** and H**3** layers (Figure 4a). The closest intermolecular distances between the two centroids of the pentafluorophenyl group in H**1** and the phenyl group in H**3** are 3.6671(8) Å [*Ring* C1-C2-C3-C4-C5-C6 (x, y, z) and *Ring* C25-C26-C27-C28-C29-C30 (x, y-1, z) indicating a weak arene–perfluoroarene interaction as shown in Figures 3a and 4a. Remarkable intermolecular interactions were observed along the *c* axis (Figure 4b); two molecules, H**1** and H**3**, are very close between the two edges of the compounds next to each other on the same plane by C-H⋯F interactions [28,31]. The corresponding distances of C20⋯F4, C23⋯F4, C30⋯F4, C29⋯F5, and C29⋯F10 are 3.418(2), 3.604(2), 3.541(2), 3.282(2), and 3.366(2) Å, respectively. Due to the CH⋯F interaction, the alternating columnar layers through arene–perfluoroarene interactions are further alternately staggered to form checkered patterns. No intermolecular hydrogen bonds are observed because of the stabilized intramolecular hydrogen bonds of each compound.
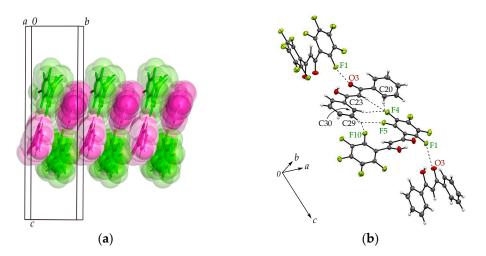

(a)   (b)

Figure 4. Packing structures of H**1**●H**3**: (**a**) the comprehensive view of the stacking structure and (**b**) major intermolecular interactions.

The molecules in the co-crystal of H$_2$**2**●H$_2$**4** have almost the same orientation (Figures 3b and 5) as the molecules in the H**1**●H**3** co-crystal (Figures 3a and 4). The bond lengths of O1-C7, O2-C9, and O3-C11 are 1.3276(16), 1.2729(16), and 1.3313(16) Å, respectively, and those of O4-C24, O5-C26, and O6-C28 are 1.3304(15), 1.2746(16), and 1.3343(16) Å, respectively. The torsional angle of the C1-C6-C7-O1 and O3-C11-C12-C13 are -29.51(17)° and 30.12(17)°, respectively, and that

of C18-C23-C24-O4 and O6-C28-C29-C30 are 16.08(17)° and -11.66(17)°, respectively. The closest intermolecular distances between the two centroids of the pentafluorophenyl group in H$_2$**2** and the phenyl group in H$_2$**4** are 3.6949(8) Å, indicating that the driving force of the co-crystal is the arene–perfluoroarene interactions in the crystal. The C-H···F intermolecular interactions were also observed in H$_2$**2**•H$_2$**4**, but the remarkable short distance was only observed in C25···F4 [3.344(2) Å].

Figure 5. Packing structure of H$_2$**2**•H$_2$**4**: (**a**) the comprehensive view of the stacking structure and (**b**) major intermolecular interactions.

For understanding the intermolecular association of the two co-crystals, density functional theory (DFT) calculations using B3LYP/6-31G* [48,49] were performed for each compound [55,56]. The electrostatic potential (ESP) surfaces for H**1**~H$_2$**4** are shown in Figure 6. Based on the orientation of the two aromatic rings of each compound, two stable structures with a bowl shape (the twisted direction of the aromatic rings is the same and the corresponding twist angle is small) and twisted shape (the twisted direction of the aromatic rings is opposite and the corresponding twist angle is large) were obtained. For example, the torsion angles of C5-C6-C10-C15 for the diketones H**1** and H**3** and C5-C6-C12-C17 for the triketones H$_2$**2** and H$_2$**4**, of which the numbering schemes are assigned in Figure 1, were calculated to be around 1° and 60° for the bowl and twisted shapes, respectively. Typically, the torsion angle of C5-C6-C10-C15 in compound H**1** is 0.13° for the bowl shape and 61.63° for the twisted shape. In the ESP, the property range of the bowl and twisted shapes are very similar to +118.3 ~ −142.1 kJ mol^{-1} and +112.6 ~ −143.8 kJ mol^{-1}, respectively. Since all the co-crystals have a bowl shape, the ESP shows only bowl shapes in Figure 6. In the map, the blue color shows electron poor regions, indicating the proton atoms and the center parts of the pentafluorophenyl groups; the highest potential energies of H**1**, H**3**, H$_2$**2**, and H$_2$**4** are +118.3, +109.6, +119.1, and +99.6 kJ mol^{-1}, respectively, of the hydroxy protons. The lowest potential energies are assigned to the oxygen atoms. The most interesting information is the inverted potential energy of the aromatic rings between the perfluorinated and non-fluorinated compounds. In the pentafluorophenyl rings of H**1** and H$_2$**2**, the higher potentials due to electron poor regions (blue color) are occupied in the aromatic center (max. +106.7 kJ mol^{-1} for H**1** and +100.2 kJ mol^{-1} for H$_2$**2**). The lower potentials due to the electron-rich regions (green–yellow color) are occupied in the edge of the fluorine atoms, and both of the F1 atoms in H**1** and H$_2$**2** shows smaller values, approximately −40 ~ −60 kJ mol^{-1}, which gives the intermolecular CH···F interactions in the co-crystals, as shown in Figures 4b and 5b. On the other hand, in the phenyl rings of H**3** and H$_2$**4**, the higher regions (blue color) are occupied on the edge of the protons (max. +104.3 kJ mol^{-1} for proton H30 bound on C30 in H**3** and +99.6 kJ mol^{-1} for the proton H34 bound to C34 in H$_2$**4**) and the lower regions (green–yellow color) are occupied in the aromatic center (min. −67.6 kJ mol^{-1} for H**3** and −63.0 kJ mol^{-1} for H$_2$**4**). These opposite electron distributions between the perfluorinated and non-fluorinated compounds indicate co-crystallizations through the arene-perfluoroarene and CH···F interactions [55,56], when two molecules approach each other.
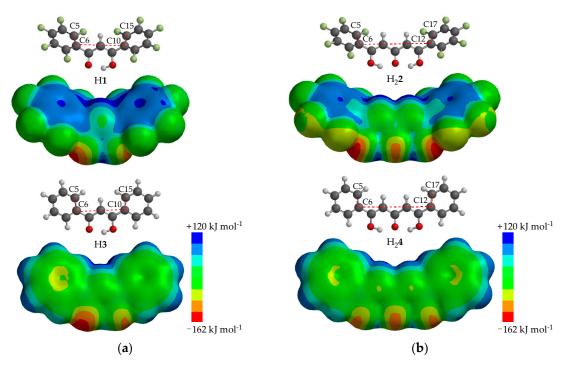
Figure 6. The energy potential maps [-162 kJ mol^{-1} (red) to $+120$ kJ mol^{-1} (blue)] of four compounds: (**a**) H**1** vs. H**3** and (**b**) H$_2$**2** vs. H$_2$**4**.

4. Conclusions

We have demonstrated arene–perfluoroarene interactions between fully-fluorinated compounds and the corresponding non-perfluorinated compounds to give alternate layered supramolecular associations in the crystal states. Two fully-fluorinated compounds, the diketone H**1** and triketone H$_2$**2**, were prepared and characterized by ^{1}H NMR, elemental analysis and X-ray crystallography. The UV-Vis spectra of H**1** and H$_2$**2** show keto-enol and enol-keto-enol structures, respectively. The compounds further interacted with the corresponding non-perfluorinated compounds to give 1:1 alternating co-crystals, which were characterized by elemental analysis and single crystal X-ray analysis. In the co-crystals, the intermolecular arene–perfluoroarene interactions were observed between the pentafluorophenyl rings and phenyl rings showing that the opposite quadrupole moments are responsible for their association as indicated by the DFT calculations.

Author Contributions: Syntheses: T.K., S.S. & K.N.; calculations, measurements and original draft preparation: T.K.; supervision: H.Y. & I.I.R.; manuscript review and editing: I.I.R & A.H.; crystal structure analysis, conceptualization, funding acquisition and project administration: A.H.

Conflicts of Interest: The authors declare no conflict of interest.

References

1. Desiraju, G.R.; Steiner, T. *The Weak Hydrogen Bond in Structural Chemistry and Biology*; IUCR, Ed.; Oxford University Press: Oxford, UK, 1999; pp. 202–224.

2. Metrangolo, P.; Neukirch, H.; Pilati, T.; Resnatti, G. Halogen bonding based recognition processes: A world parallel to hydrogen bonding. *Acc. Chem. Res.* **2005**, *38*, 386–395. [CrossRef]

3. Shimizu, K.; Ferreira da Silva, J. Halogen and hydrogen bonding interplay in the crystal packing of halometallocenes. *Molecules* **2018**, *23*, 2959. [CrossRef] [PubMed]

4. Itoh, T.; Kondo, M.; Kanaikea, M.; Masaoka, S. Arene–perfluoroarene interactions for crystal engineering of metal complexes: Controlled self-assembly of paddle-wheel dimers. *CrystEngComm* **2013**, *15*, 6122–6126. [CrossRef]

5. Bouyahyi, M.; Roisnel, T.; Carpentier, J.-F. Aluminum complexes of fluorinated β-diketonate ligands: Syntheses, structures, intramolecular reduction, and use in ring-opening polymerization of lactide. *Organometallics* **2010**, *29*, 491–500. [CrossRef]

6. Hernández-Trujillo, J.; Vela, A. Molecular quadrupole moments for the series of fluoro- and chlorobenzenes. *J. Phys. Chem.* **1996**, *100*, 6524–6530. [CrossRef]

7. Doerksen, R.J.; Thakkar, A.J. Quadrupole and octopole moments of heteroaromatic rings. *J. Phys. Chem. A* **1999**, *103*, 10009–10014. [CrossRef]

8. Williams, J.H. The molecular electric quadrupole moment and solid-state architecture. *Acc. Chem. Res.* **1993**, *26*, 593–598. [CrossRef]

9. Patrick, C.R.; Prosser, G.S. A molecular complex of benzene and hexafluorobenzene. *Nature* **1960**, *187*, 1021. [CrossRef]

10. Hori, A. *The importance of π-interactions in crystal enigineering*; Tiekink, E.R., Zukerman-Schpector, J., Eds.; John Wiley & Sons: Hoboken, NJ, USA, 2012; pp. 163–185.

11. Salonen, L.M.; Ellermann, M.; Diederich, F. Aromatic rings in chemical and biological recognition: Energetics and structures. *Angew. Chem. Int. Ed.* **2011**, *50*, 4808–4842. [CrossRef]

12. Coates, G.W.; Dunn, A.R.; Henling, L.M.; Dougherty, D.A.; Grubbs, R.H. Phenyl-perfluorophenyl stacking interactions: A new strategy for supermolecule construction. *Angew. Chem. Int. Ed. Engl.* **1997**, *36*, 248–251. [CrossRef]

13. Kilbinger, A.F.M.; Grubbs, R.H. Arene-perfluoroarene interactions as physical crosslinks for hydrogel formation. *Angew. Chem. Int. Ed.* **2002**, *41*, 1563–1566. [CrossRef]

14. Vangala, V.R.; Nangia, A.; Lynch, V.M. Interplay of phenyl-perfluorophenyl stacking, C-H⋯F, C-F⋯π and F⋯F interactions in some crystalline aromatic azines. *Chem. Commun.* **2002**, 1304–1305. [CrossRef]

15. Reichenbächer, K.; Süss, H.I.; Hulliger, J. Fluorine in crystal engineering—"The little atom that could". *Chem. Soc. Rev.* **2005**, *34*, 22–30. [CrossRef] [PubMed]

16. Xu, R.; Gramlich, V.; Frauenrath, H. Alternating diacetylene copolymer utilizing perfluorophenyl-phenyl interactions. *J. Am. Chem. Soc.* **2006**, *128*, 5541–5547. [CrossRef]

17. Dai, C.; Nguyen, P.; Marder, T.B.; Scott, A.J.; Clegg, W.; Viney, C. Control of single crystal structure and liquid crystal phase behaviour via arene-perfluoroarene interactions. *Chem. Commun.* **1999**, 2493–2494. [CrossRef]

18. Collings, J.C.; Roscoe, K.P.; Robins, E.G.; Batsanov, A.S.; Stimson, L.M.; Howard, J.A.K.; Clark, S.J.; Marder, T.B. Arene-perfluoroarene interactions in crystal engineering. 8: Structures of 1:1 complexes of hexafluorobenzene with fused-ring polyaromatic hydrocarbons. *New J. Chem.* **2002**, *26*, 1740–1746. [CrossRef]

19. Fasina, T.M.; Collings, J.C.; Lydon, D.P.; Albesa-Jove, D.; Batsanov, A.S.; Howard, J.A.K.; Nguyen, P.; Bruce, M.; Scott, A.J.; Clegg, W.; et al. Synthesis, optical properties, crystal structures and phase behaviour of selectively fluorinated 1,4-bis(4′-pyridylethynyl)benzenes, 4-(phenylethynyl)pyridines and 9,10-bis(4′-pyridylethynyl)anthracene, and a $Zn(NO_3)_2$ coordination polymer. *J. Mater. Chem.* **2004**, *14*, 2395–2404. [CrossRef]

20. Collings, J.C.; Batsanov, A.S.; Howard, J.A.K.; Dickie, D.A.; Clyburne, J.A.C.; Jenkins, H.A.; Marder, T.B. 1:1 Complexes of octafluoronaphthalene with trans-stilbene and trans-azobenzene. *J. Fluor. Chem.* **2005**, *126*, 515–519. [CrossRef]

21. Batsanov, A.S.; Collings, J.C.; Marder, T.B. Arene-perfluoroarene interactions in crystal engineering. XV. Ferrocene-decafluorobiphenyl (1/1). *Acta Cryst.* **2006**, *C62*, m229–m231. [CrossRef]

22. Vigato, P.A.; Peruzzo, V.; Tamburini, S. The evolution of β-diketone or β-diketophenol ligands and related complexes. *Coord. Chem. Rev.* **2009**, *253*, 1099–1201. [CrossRef]

23. Haneline, M.R.; Tsunoda, M.; Gabbaï, F.P. π-Complexation of biphenyl, naphthalene, and triphenylene to trimeric perfluoro-ortho-phenylene mercury. Formation of extended binary stacks with unusual luminescent properties. *J. Am. Chem. Soc.* **2002**, *124*, 3737–3742. [CrossRef]

24. Taylor, T.J.; Bakhmutov, V.I.; Gabbaï, F.P. Hydrocarbon uptake in the alkylated micropores of a columnar supramolecular solid. *Angew. Chem. Int. Ed.* **2006**, *45*, 7030–7033. [CrossRef]

25. Taylor, T.J.; Gabbaï, F.P. Supramolecular stabilization of α,ω-diphenylpolyynes by complexation to the tridentate lewis acid [o-C_6F_4Hg]$_3$. *Organometallics* **2006**, *25*, 2143–2147. [CrossRef]

26. Gunawardana, C.A.; Aakeröy, C.B. Co-crystal synthesis: Fact, fancy, and great expectations. *Chem Commun.* **2018**, *54*, 14047–14060. [CrossRef]

27. Maiti, B.; Bhattacharjee, S.; Bhattacharya, S. Perfluoroarene induces a pentapeptidic hydrotrope into a pH-tolerant hydrogel allowing naked eye sensing of Ca^{2+} ions. *Nanoscale* **2019**, *11*, 2223–2230. [CrossRef]

28. Thalladi, V.R.; Weiss, H.-C.; Blaser, D.; Boese, R.; Nangia, A.; Desiraju, G.R. C-H···F interactions in the crystal structures of some fluorobenzenes. *J. Am. Chem. Soc.* **1998**, *120*, 8702–8710. [CrossRef]

29. Ferreira da Silva, J.L.; Shimizu, K.; Duarte, M.T. The role of halogen interactions in the crystal structure of biscyclopentadiethnyl dihalides. *CrystEngComm* **2017**, *19*, 2802–2812. [CrossRef]

30. Marushima, Y.; Uchiumi, Y.; Ogua, K.; Hori, A. Intermolecular π-stacking and F···F interactions of fluorine-substituted meso-alkynylporphyrin. *Acta Cryst.* **2010**, *C66*, o406–o409.

31. Hori, A.; Shinohe, A.; Yamasaki, M.; Nishibori, E.; Aoyagi, S.; Sakata, M. 1:1 Cross-assembly of two β-diketonate complexes through arene-perfluoroarene interactions. *Angew. Chem. Int. Ed.* **2007**, *46*, 7617–7620. [CrossRef] [PubMed]

32. Hori, A.; Arii, T. Cation-π and arene-perfluoroarene interactions between Cu(II) fluorine-substituted β-diketonate complex and benzenes. *CrystEngComm* **2007**, *9*, 215–217. [CrossRef]

33. Hori, A.; Takatani, S.; Miyamoto, T.K.; Hasegawa, M. Luminescence from π–π stacked bipyridines through arene–perfluoroarene interactions. *CrystEngComm* **2009**, *11*, 567–569. [CrossRef]

34. Hori, A.; Nakajima, K.; Akimoto, Y.; Naganuma, K.; Yuge, H. Guest-adjusted encapsulation and thermal studies of non-porous mononuclear Cu(II) coordination complexes through electrostatic interactions induced by fluorine substitution. *CrystEngComm* **2014**, *16*, 8805–8817. [CrossRef]

35. Hori, A.; Gonda, R.; Rzeznicka, I.I. Enhanced adsorption of small gas molecules in metal (Cu^{2+}, Pd^{2+}, Pt^{2+}) complexes induced by ligand fluorination. *CrystEngComm* **2017**, *19*, 6263–6266. [CrossRef]

36. Hori, A.; Shinohe, A.; Takatani, S.; Miyamoto, T.K. Synthesis and crystal structures of fluorinated β-diketonate metal (Al^{3+}, Co^{2+}, Ni^{2+}, and Cu^{2+}) complexes. *Bull. Chem. Soc. Jpn.* **2009**, *82*, 96–98. [CrossRef]

37. Ma, B.-Q.; Gao, S.; Wang, Z.-M.; Liao, C.-S.; Yan, C.-H.; Xu, G.-X. Synthesis and structure of bis(dibenzoylmethanato)copper(II). *J. Chem. Cryst.* **1999**, *29*, 793–796. [CrossRef]

38. Morita, H.; Nakanishi, H. Electronic structure and spectra of the enol form of some β-diketones. *Bull. Chem. Soc. Jpn.* **1981**, *54*, 378–386. [CrossRef]

39. Moriyasu, M.; Kato, A.; Hashimoto, Y. Kinetic studies of fast equilibrium by means of high-performance liquid chromatography. Part 11. Keto-enol tautomerism of some β-dicarbonyl compounds. *J. Chem. Soc. Perkin Trans.* **1986**, *2*, 515–520. [CrossRef]

40. Bertolasi, V.; Gilli, P.; Ferretti, V.; Gilli, G. Evidence for resonance-assisted hydrogen bonding. 2. Intercorrelation between crystal structure and spectroscopic parameters in eight intramolecularly hydrogen bonded 1,3-diaryl-1,3-propanedione enols. *J. Am. Chem. Soc.* **1991**, *113*, 4917–4925. [CrossRef]

41. Gilli, P.; Bertolasi, V.; Pretto, L.; Ferretti, V.; Gilli, G. Covalent versus electrostatic nature of the strong hydrogen bond: discrimination among single, double, and asymmetric single-well hydrogen bonds by variable-temperature X-ray crystallographic methods in β-diketone enol RAHB systems. *J. Am. Chem. Soc.* **2004**, *126*, 3845–3855. [CrossRef]

42. Tobita, S.; Ohba, J.; Nakagawa, K.; Shizuka, H. Recovery mechanism of the reaction intermediate produced by photoinduced cleavage of the intramolecular hydrogen bond of dibenzoylmethane. *J. Photochem. Photobiol. A Chem.* **1995**, *92*, 61–67. [CrossRef]

43. Cantrell, A.; McGarvey, D.J. Photochemical studies of 4-tert-butyl-4′-methoxydibenzoylmethane (BM-DBM). *J. Photochem. Photobiol. B Biol.* **2001**, *64*, 117–122. [CrossRef]

44. Nagashima, N.; Kudoh, S.; Takayanagi, M.; Nakata, M. UV-induced photoisomerization of acetylacetone and identification of less-stable isomers by low-temperature matrix-isolation infrared spectroscopy and density functional theory calculation. *J. Phys. Chem. A* **2001**, *105*, 10832–10838. [CrossRef]

45. Wiechmann, M.; Port, H.; Frey, W.; Laermer, F.; Elsaesser, T. Time-resolved spectroscopy on ultrafast proton transfer in 2-(2′-hydroxy-5′-methylphenyl)benzotriazole in liquid and polymer environments. *J. Phys. Chem.* **1991**, *95*, 1918–1923. [CrossRef]

46. Ünver, H.; Kabak, M.; Zengin, D.M.; Durlu, T.N. Keto-enal tautomerism, conformations, and structure of 1-[N-(4-chlorophenyl)]aminomethhylidene-2(1H)naphthalenone. *J. Chem. Crystallogr.* **2001**, *31*, 203–209. [CrossRef]

47. Claramunt, R.M.; López, C.; María, M.D.S.; Sanz, D.; Elguero, J. The use of NMR spectroscopy to study tautomerism. *Prog. Nucl. Magn. Reson. Spectrosc.* **2006**, *49*, 169–206. [CrossRef]

48. Becke, A.D. Density-functional thermochemistry. III. The role of exact exchange. *J. Chem. Phys.* **1993**, *98*, 5648–5652. [CrossRef]
49. Lee, C.; Yang, W.; Parr, R.G. Development of the Colle-Salvetti correlation-energy formula into a functional of the electron density. *Phys. Rev. B* **1988**, *37*, 785–789. [CrossRef]
50. Filler, R.; Rao, Y.S.; Biezais, A.; Miller, F.N.; Beaucaire, V.D. Polyfluoroaryl β-dicarbonyl compounds. *J. Org. Chem.* **1970**, *35*, 930–935. [CrossRef]
51. Sheldrick, G.M. SHELXT—Integrated space-group and crystal-structure determination. *Acta Cryst.* **2015**, *A71*, 3–8. [CrossRef]
52. Sheldrick, G.M. Crystal structure refinement with SHELXL. *Acta Cryst.* **2015**, *C71*, 3–8.
53. Thomas, L.H.; Florence, A.J.; Wilson, C.C. Hydrogen atom behavior imaged in a short intramolecular hydrogen bond using the combined approach of X-ray and neutron diffraction. *New. J. Chem.* **2009**, *33*, 2486–2490. [CrossRef]
54. Cea-Olivares, R.; Rodriguez, I.; Rosales, M.J.; Toscano, R.A. The structure of triketones in the solid sate. The crystal structure of 1,5-diphenylpentane-1,3,5-trione. *Aust. J. Chem.* **1987**, *40*, 1127–1130. [CrossRef]
55. Wheeler, S.E. Local nature of Substituent effects in stacking interactions. *J. Am. Chem. Soc.* **2011**, *133*, 3687–3689. [CrossRef] [PubMed]
56. Ringer, A.L.; Sherrill, C.D. Substituent Effects in Sandwich Configurations of Multiply Substituted Benzene Dimers Are Not Solely Governed By Electrostatic Control. *J. Am. Chem. Soc.* **2009**, *131*, 4574–4575. [CrossRef] [PubMed]